Additional File 1

1. Fig. S1. m^6A methylation in *Arabidopsis* and *Oryza sativa*.

2. Fig. S2. m^6A methylation deposits in the 5’ UTR of mRNA shifted H3K4me3 histone modification.

3. Fig. S3. Genotyping of T-DNA insertion mutants and m^6A levels in different plants.

4. Fig. S4. The negative control of MTA and ATX1 interact with CTD of RNA Pol II.

5. Fig. S5. The diagram to show the T-DNA insertion for *alkbh10b-1*.

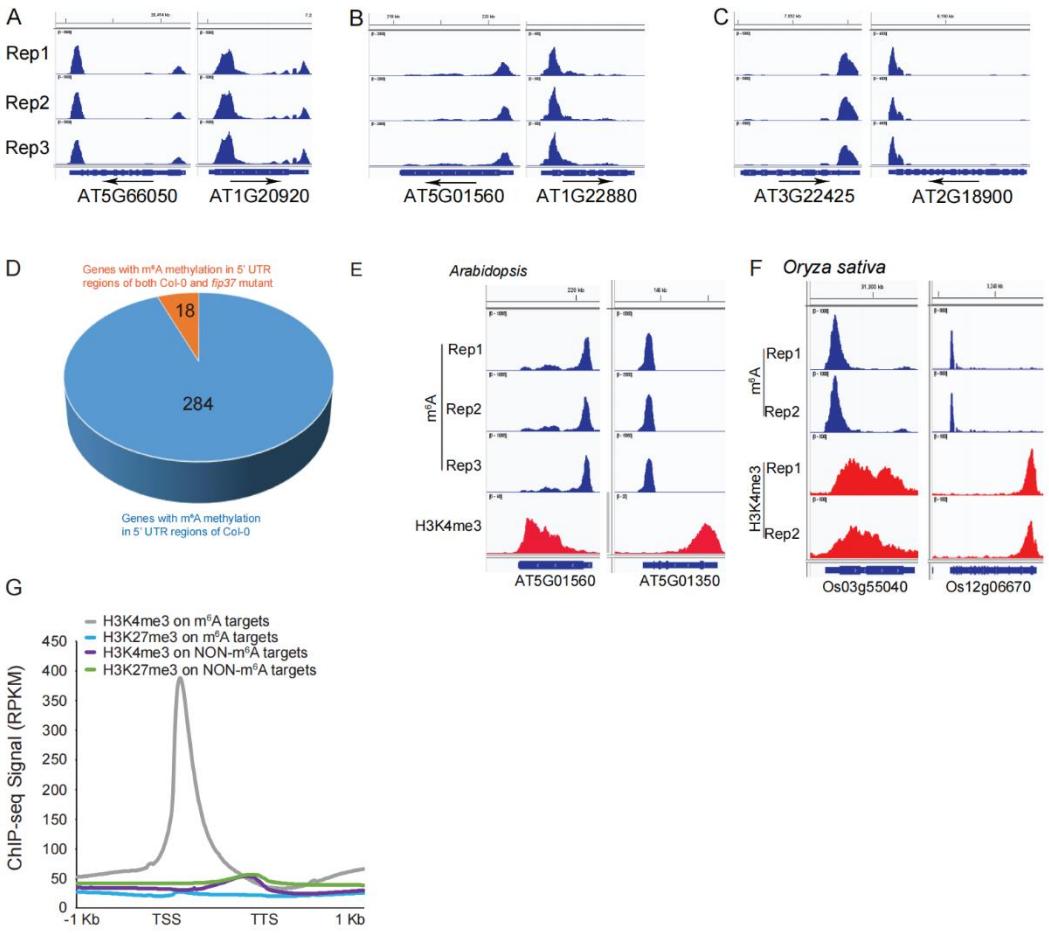

Fig. S1. m^{6}A methylation in *Arabidopsis* and *Oryza sativa*. **A-C** Genes with m^{6}A methylation in both 5' UTR and 3' UTR region (m^{6}A$_{53}$) (**A**), genes with m^{6}A methylation only in 5' UTR region (m^{6}A$_5$) (**B**) and genes with m^{6}A methylation only in 3' UTR region (m^{6}A$_3$) (**C**) were shown. **D** The genes with m^{6}A modification in 5' UTR regions uniquely detected in Col-0 (blue), and shared with *fip37* mutant (orange). **E** Genome browser traces of m^{6}A-seq and H3K4me3 ChIP-seq data from representative genes in *Arabidopsis*. **F** Genome browser traces of m^{6}A-seq and H3K4me3 ChIP-seq data from representative genes in *Oryza sativa*. **G** Distribution of H3K4me3 or H3K27me3 reads in transcript segments with or without m^{6}A modification.

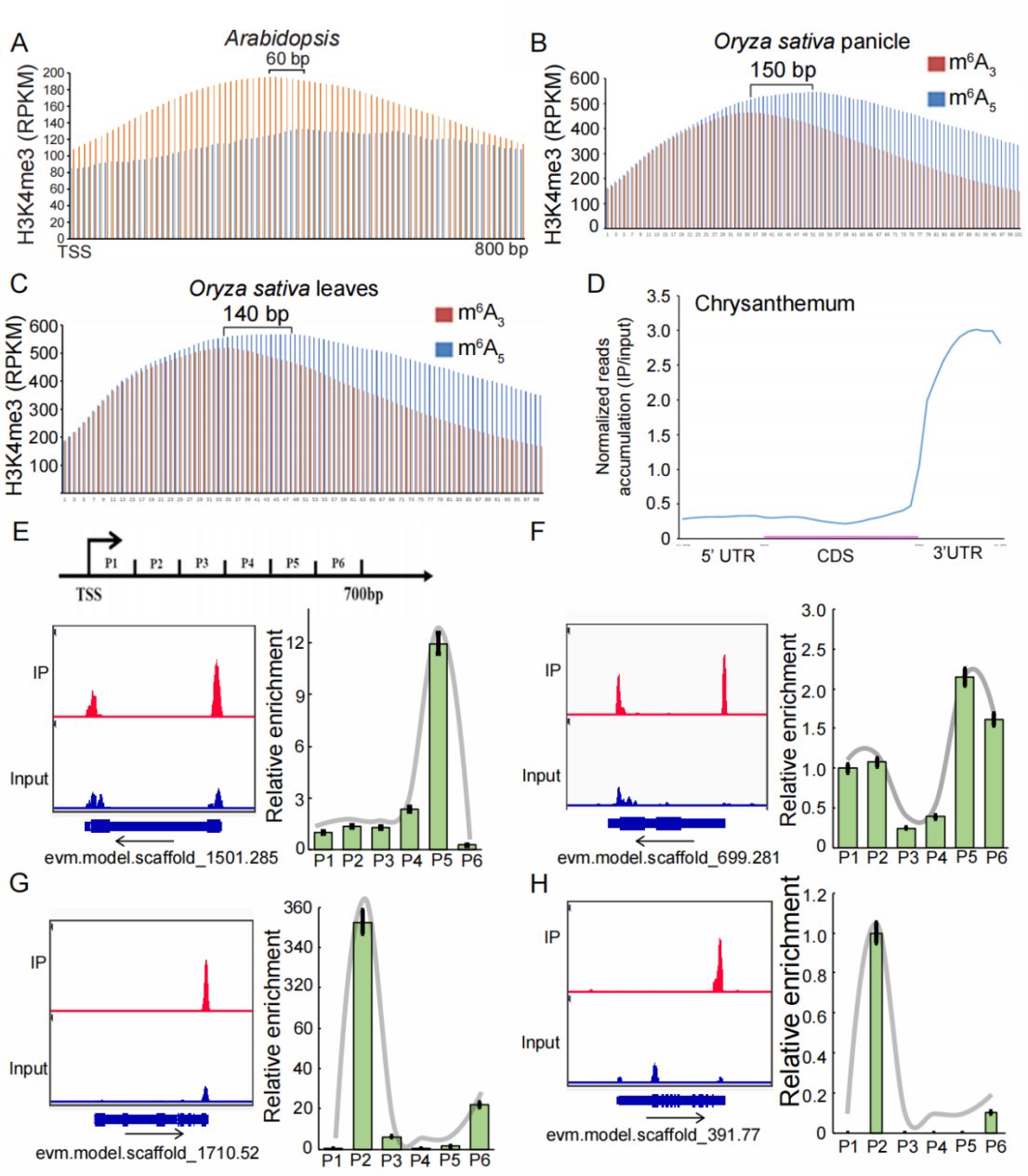

Fig. S2. m^{6}A methylation deposits in the 5' UTR of mRNA shifted H3K4me3 histone modification. **A-C** Bar plots show the normalized H3K4me3 signal downstream of TSS in leaves of *Arabidopsis* (**A**), panicle (**B**) and leaves (**C**) of *Oryza sativa*. Normalized H3K4me3 signal downstream of the TSS were binned in 10-bp intervals, and the distribution was plotted. The distance between summits was indicated in the figure. m^{6}A$_3$: genes with m^{6}A methylation only in 3' UTR region; m^{6}A$_5$: genes with m^{6}A methylation only in 5' UTR region. **D** Accumulation of m^{6}A-IP reads along transcripts in chrysanthemum. Each transcript was divided into three parts: 5' UTRs, CDS and 3' UTRs. **E-H** Genome browser traces and ChIP-qPCR to show the m^{6}A enrichment and H3K4me3 modification, respectively, for genes with m^{6}A modification specifically in 5' UTR regions (**E-F**) and 3' UTR regions (**G-H**). About 700 bp regions were divided into 6 parts for ChIP-qPCR examination.

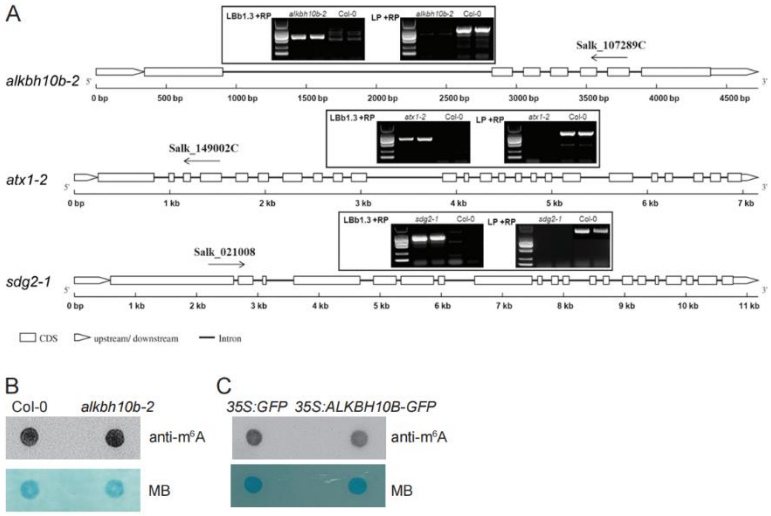

Fig. S3. Genotyping of T-DNA insertion mutants and m^{6}A levels in different plants. **A** The diagram to show the T-DNA insertion for *alkbh10b-2*, *atx1-2* and *sdg2-1* mutants. Genotyping results were shown. **B-C** m^{6}A dot-blot assay to illustrate the overall level variances between Col-0 and *alkbh10b-2* mutant (**B**), and the global change in m^{6}A modification in cells expressing *35S:AtALKBH10B-GFP* (**C**).

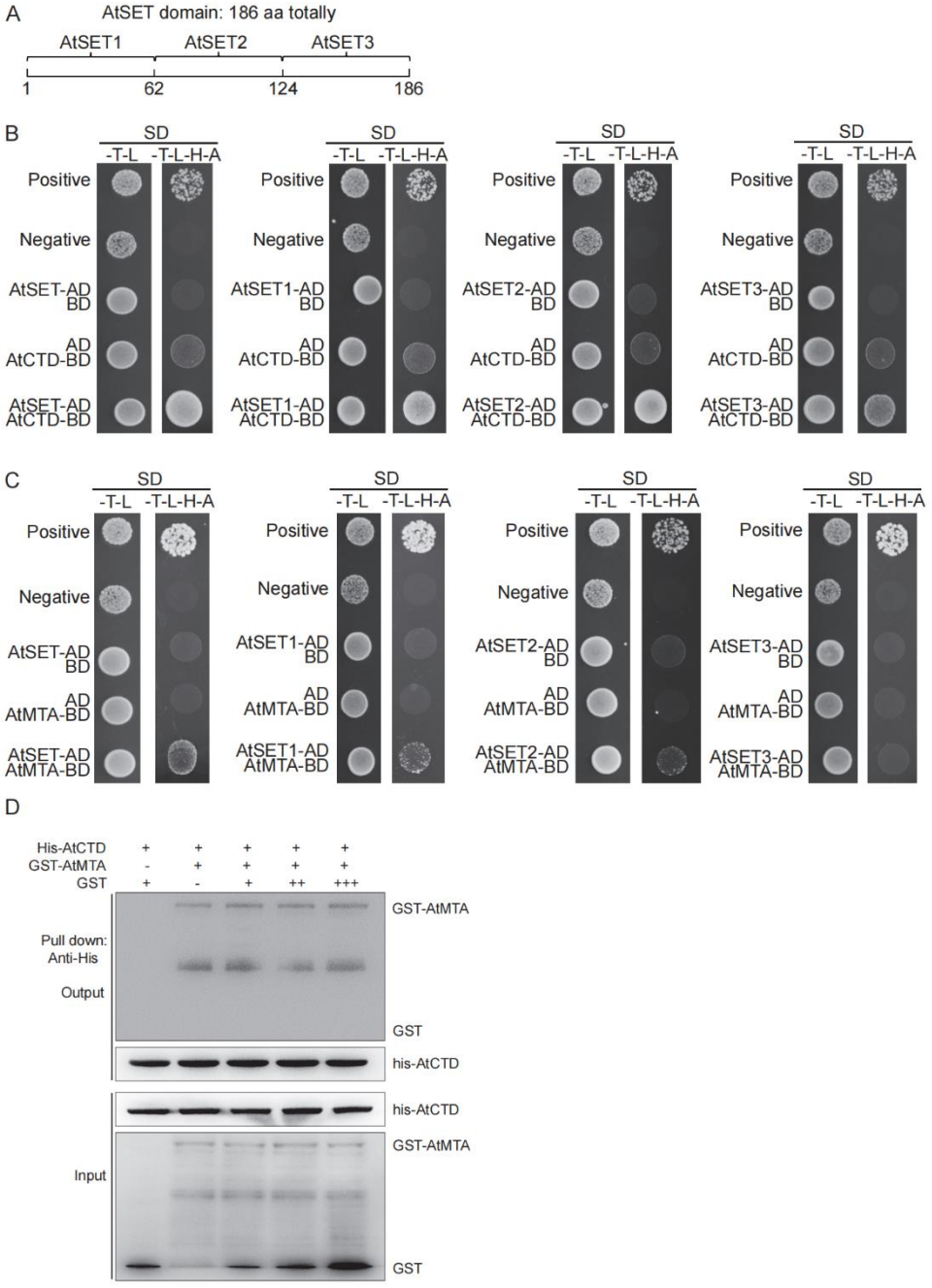

Fig. S4. The negative control of MTA and ATX1 interact with CTD of RNA Pol II. **A** The diagram to show the 3 fragments of AtSET domain (AtSET1-3) used for the following assays. **B-C** Y2H assay indicates the interaction between AtCTD and AtSET fragments (**B**), as well as between AtMTA and AtSET fragments (**C**). **D** Pull-down assays to examine the interaction between GST or AtMTA and AtCTD. Increasing concentrations of GST was respectively incubated with a fixed concentration of GST-AtMTA. GST-fusion proteins and GST were detected with an anti-GST antibody. Input means total protein lysate without immunoprecipitation.

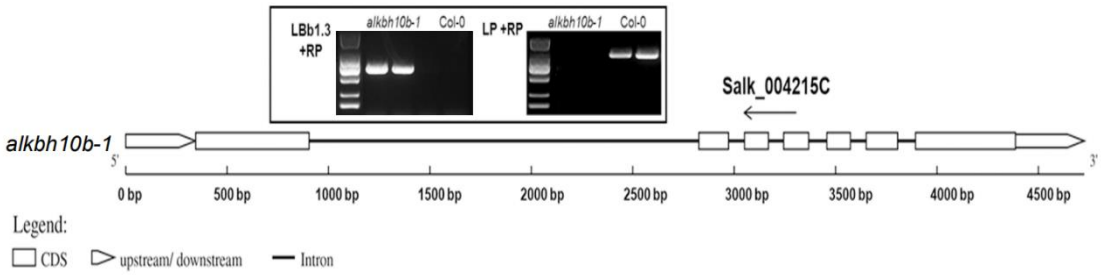

Fig. S5. The diagram to show the T-DNA insertion for *alkbh10b-1*. Genotyping results were shown.